RNA (1998), *4*:1282–1294. Cambridge University Press. Printed in the USA.

Metal ion probing of rRNAs: Evidence for evolutionarily conserved divalent cation binding pockets

NORBERT POLACEK and ANDREA BARTA
Institute of Biochemistry, University of Vienna, Vienna Biocenter, Dr. Bohr-Gasse 9/3, A-1030 Vienna, Austria

ABSTRACT

Ribosomes are multifunctional RNP complexes whose catalytic activities absolutely depend on divalent metal ions. It is assumed that structurally and functionally important metal ions are coordinated to highly ordered RNA structures that form metal ion binding pockets. One potent tool to identify the structural surroundings of high-affinity metal ion binding pockets is metal ion-induced cleavage of RNA. Exposure of ribosomes to divalent metal ions, such as Pb^{2+}, Mg^{2+}, Mn^{2+}, and Ca^{2+}, resulted in site-specific cleavage of rRNAs. Sites of strand scission catalyzed by different cations accumulate at distinct positions, indicating the existence of general metal ion binding centers in the highly folded rRNAs in close proximity to the cleavage sites. Two of the most efficient cleavage sites are located in the 5′ domain of both 23S and 16S rRNA, regions that are known to self-fold even in the absence of ribosomal proteins. Some of the efficient cleavage sites were mapped to the peptidyl transferase center located in the large ribosomal subunit. Furthermore, one of these cleavages was clearly diminished upon AcPhe-tRNA binding to the P site, but was not affected by uncharged tRNA. This provides evidence for a close physical proximity of a metal ion to the amino acid moiety of charged tRNAs. Interestingly, comparison of the metal ion cleavage pattern of eubacterial 70S with that of human 80S ribosomes showed that certain cleavage sites are evolutionarily highly conserved, thus demonstrating an identical location of a nearby metal ion. This suggests that cations, bound to evolutionarily constrained binding sites, are reasonable candidates for being of structural or functional importance.

Keywords: metal ion catalysis; metal ion cleavage; peptidyl transferase; rRNA structure

INTRODUCTION

Ribosomes have to deal with the problem of packing RNA secondary structure elements specifically into highly ordered complexes capable of deciphering the genetic code. Positively charged ions, including polyamines, monovalent ions, and divalent metal ions, are strictly required for counterbalancing electrostatic repulsion of the polyanionic RNA and for promoting fine tuning of rRNA structures (reviewed in Streicher & Wallis, 1996). In general, nonspecific ion–RNA interactions, in which the cations are not well localized, contrast with highly specific binding of metal ions to defined binding pockets. Divalent metal ions are known to promote nucleic acid folding and can even participate directly in RNA catalysis (Pan et al., 1993).

In the last few years, much has been learned about the architecture of specific metal ion binding sites in structured RNA molecules. High-resolution structure analysis of ribozymes and RNA domains revealed motifs for metal ion binding pockets in the major groove near local perturbations of the helix caused by noncanonical base pairs, loops, and bulges. The identified ion-binding motifs were shown to be created by tandem G·U wobble pairs (Allain & Varani, 1995; Cate & Doudna, 1996) or by a G-C base pair followed by a sheared G·A pair (Pley et al., 1994; Scott et al., 1995; Baeyens et al., 1996). Interestingly, comparative sequence analysis showed that these sequence motifs are highly conserved and frequently found in rRNAs (Gautheret et al., 1994, 1995), suggesting specific metal ion coordination in the ribosome. Most recently, metal ion binding sites in the crystal structure of a 5S rRNA domain were identified that were located in the major groove at novel RNA motifs termed “cross-strand purine stacks” and at three noncanonical base pairs forming a “metal zipper” (Correll et al., 1997). However, no structural information about metal ion binding sites within the 16S and 23S rRNAs have been described so far.

All RNA-catalyzed reactions known to date either require or are greatly stimulated by divalent metal ions,

Reprint requests to: Andrea Barta, Institute of Biochemistry, University of Vienna, Vienna Biocenter, Dr. Bohr-Gasse 9/3, A-1030 Vienna, Austria; e-mail: andrea@bch.univie.ac.at.

which can play structural roles or participate directly in RNA catalysis (Pan et al., 1993). There is accumulating evidence that many, if not all, activities of the ribosome are RNA mediated. Most convincingly, peptide bond formation is catalyzed in a compartment that was shown to be predominantely composed of RNA (Steiner et al., 1988) and turned out to be resistant to partial ribosomal protein extraction procedures but is sensitive to RNase or EDTA treatment (Noller et al., 1992). Taken together, these data support the hypothesis that parts of the rRNAs are involved in the main enzymatic reaction of the ribosome and it has been proposed that specifically coordinated divalent metal ions may participate in catalysis (Barta & Halama, 1996; Winter et al., 1997). That RNA has the potential of catalyzing peptide bond formation in an Mg^{2+}-dependent manner was demonstrated recently by in vitro-selected ribozymes (Zhang & Cech, 1997). Strong evidence for the hypothesis of an rRNA-catalyzed peptide bond formation on the ribosome was published very recently by Watanabe and coworkers, who reported that an in vitro transcript of 23S rRNA has intrinsic peptidyl transferase activity (Nitta et al., 1998).

In the absence of high-resolution ribosome crystal structures, indirect methods must be applied to obtain insight into the fine structure of the well-ordered rRNAs and their high-affinity metal ion binding sites. Due to its 2′-OH group, RNA is sensitive to metal ion-mediated hydrolysis. Recent studies demonstrated that highly efficient cleavage sites within folded RNA molecules correspond to structurally adjacent metal binding sites (Kazakov & Altman, 1991; Pan et al., 1993; Streicher et al., 1993; Zito et al., 1993). Specific metal ion hydrolysis in combination with other experimental probing data allowed the positioning of two Mg^{2+} ions near the catalytic core of a group I ribozyme in the context of a 3D model (Streicher et al., 1996). The best understood metal ion-catalyzed cleavage reaction is the Pb^{2+}-induced hydrolysis of yeast $tRNA^{Phe}$ (Brown et al., 1983, 1985). At a pH close to the pK_a value, the lead hydrate exists in a partially deprotonated form and extracts the proton from the 2′OH of the ribose at the cleavage site, followed by a nucleophilic attack of the 2′-O^- at the adjacent phosphodiester bond, leading to strand scission. It is noteworthy that only a limited number of bound metal ions comply with these structural features and hence can be detected with this method.

In a previous paper, we have used this method to identify highly efficient Pb^{2+} cleavage sites in the rRNAs of eubacterial 70S ribosomes (Winter et al., 1997). Competition experiments with other divalent metal ions, such as Mg^{2+}, Mn^{2+}, Ca^{2+}, or Zn^{2+}, demonstrated that Pb^{2+} cleavage could be inhibited. These experiments not only confirmed the existance of high-affinity Pb^{2+} binding sites, but also led us to speculate that Pb^{2+} ions were bound to general metal ion binding centers in the ribosome. The purpose of the work described here is to characterize more precisely the immediate environment of the proposed general ion binding sites. We also focus on weak Pb^{2+} cleavage sites and apply further specific metal ion cleavage of rRNAs with Mg^{2+}, Mn^{2+}, and Ca^{2+}, which are known to promote ribosome catalysis (Weiss et al., 1973) and to inhibit Pb^{2+} cleavages (Winter et al., 1997). Finally, we address the fundamental question whether cation binding pockets in ribosomes are conserved in evolution, because this is a prerequisite for the involvement of metal ions in peptidyl transfer.

RESULTS

Metal ion cleavage of *Escherichia coli* ribosomes

Using active ribosome particles, we investigate here the sensitivity of 23S and 16S rRNAs to site-specific hydrolysis catalyzed by different divalent metal ions such as Pb^{2+}, Mg^{2+}, Mn^{2+}, and Ca^{2+}. In general, the metal ion cleavage reaction is pH dependent, suggesting the involvement of metal hydroxides as the nucleophile during cleavage (Kazakov & Altman, 1991; Pan et al., 1994; Winter et al., 1997). Thus, the cleavage reaction was performed at a pH close to the pK_a value of the hydrated metal ion used (pK_a values are 7.7 for Pb^{2+}, 10.6 for Mn^{2+}, 11.4 for Mg^{2+} and 12.9 for Ca^{2+}). In contrast to the Pb^{2+} cleavage reaction that was performed at neutral pH, the cleavage reactions catalyzed by the other metal ions were performed at elevated pH values (pH 8 for Mn^{2+}, and pH 9 for Mg^{2+} and Ca^{2+}). These pH values lie within the known pH optimum for peptide bond formation (pH 8–9.1) (Maden & Monro, 1968; Pestka, 1972) and therefore ensure the probing of active ribosome structures. Sites of strand scission were mapped by primer extension analysis; the cleaved phosphodiester bond is always located 5′ of the indicated nucleotide. Strong, intermediate, and weak cleavage sites were defined as having more than 20-fold, between 5- and 20-fold, and less than 5-fold increased signal strength of the cleavage band compared to the corresponding band in uncleaved rRNA. The designed set of primers enabled us to scan the entire 16S and 23S rRNAs, except their 3′ ends (nt 1507–1542 on the 16S rRNA and 2886–2904 on the 23S rRNA, respectively).

Metal ion cleavages in the 23S rRNA

The strongest cleavage site in the 23S rRNA was identified at position A505 in domain I at which Pb^{2+}, Mg^{2+}, Mn^{2+}, and Ca^{2+} all hydrolyze the backbone with high yield; Ca^{2+} was the most efficient (Fig. 1A). The identical cleavage position observed with all divalent metal ions tested supports our earlier proposal (Winter et al.,

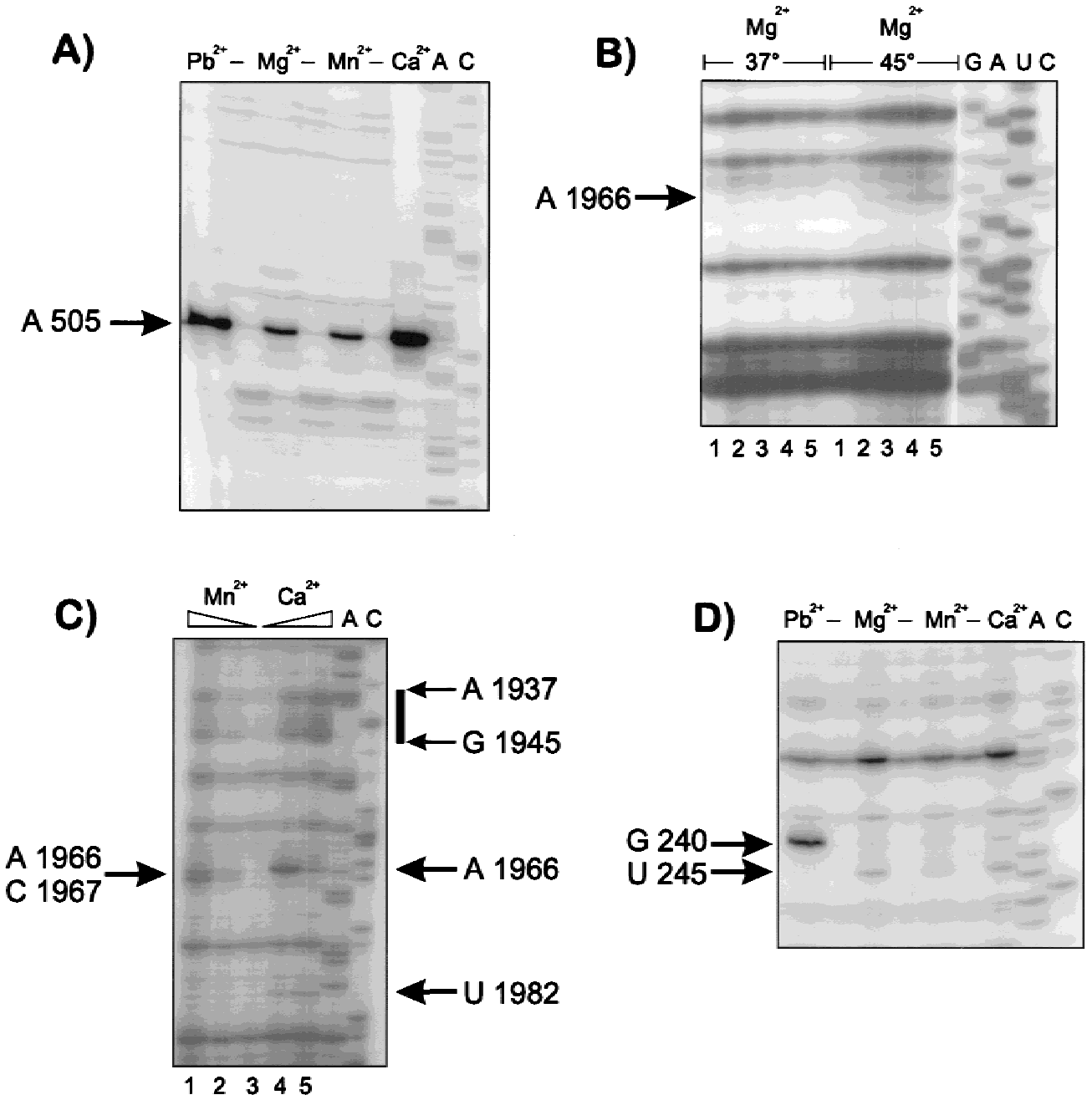

FIGURE 1. Mapping of divalent metal ion cleavage sites on rRNAs of *E. coli* by primer extension analysis. **A:** Identification of a specific site in domain I of 23S rRNA cleaved by the indicated metal ions (10 mM). The cleavage reactions were performed as described in Materials and Methods for 4 min (Pb^{2+}), 135 min (Mg^{2+}), or 60 min (Mn^{2+}, Ca^{2+}), respectively. Lanes designated (−) indicate the reverse transcription of uncleaved rRNA. **B:** Identification of a Mg^{2+} cleavage site in domain IV of 23S rRNA. 70S ribosomes were incubated with 10 mM $MgCl_2$ at pH 9 at 37 °C or 45 °C for 0, 15, 45, or 135 min (lanes 1–5). **C:** Mapping of Mn^{2+} and Ca^{2+} cleavage sites in domain IV of 23S rRNA. The rRNA was cleaved with 15 and 10 mM $MnCl_2$ (lanes 1–2) or with 10 and 15 mM $CaCl_2$ (lanes 4–5). Lane 3 shows the reverse transcription reaction of control ribosomes incubated at pH 9. Bar at right side indicates a stretch of adjacent Ca^{2+} cleavages. **D:** Identification of two cleavage sites in the 5′ domain of 16S rRNA. Cleavage reactions were performed as in A. AC and GAUC denote sequencing lanes.

1997) that this region of domain I contains one general ion binding center at or close to A505. In addition to this strong cut, a weaker Mn^{2+} and Ca^{2+} cleavage at position G406 in domain I was identified (Fig. 2A).

Domain II of the 23S rRNA was specifically hydrolyzed by Mg^{2+} at positions U653 and A654, whereas Mn^{2+} and Ca^{2+} created cuts at A654 and A655 (Fig. 2A). Three weak Pb^{2+} cleavages could be mapped to posi-

tions G785, A792, and G1026, with the latter site also being cleaved by Mn^{2+}- and Ca^{2+}-hydroxides. Interestingly, in the GTPase center of the ribosome (positions 1051–1109), which binds Mg^{2+} specifically for structure stabilization purposes (Laing et al., 1994; Xing & Draper, 1995), no metal cleavages could be observed. This reflects the limitation of this method, because only those bound metal ions catalyze cleavage whose hydroxyl group points to a structural adjacent phosphodiester bond that is in a favorable structural conformation for hydrolysis.

The region between nt 1450 and 1555 of domain III was multiply targeted by divalent metal ions, with magnesium being the most frequent (Fig. 2A). The sites of Mg^{2+}-cleavage were mapped to positions G1452, C1461, A1494, G1510, G1511, G1524, G1537, G1538, A1544, and G1555. Pb^{2+}, Mn^{2+}, and Ca^{2+} also promoted hydrolysis at some of the aforementioned sites (Pb^{2+}: U1523, U1524, G1537, G1555; Mn^{2+} and Ca^{2+}: A1494, U1523, G1524, and G1555) (Fig. 2A). No other region of 23S or 16S rRNAs was cleaved with an intensity comparable to that found in this part of domain III, suggesting that this region is easily accessible to metal ions and may be located at the surface of the ribosome.

The strongly conserved domain IV of the 23S rRNA, a part of the peptidyl transferase center, was also sensitive to metal ion-directed RNA hydrolysis. With Mg^{2+} at 45 °C, a single prominent cleavage at A1966 was identified (Fig. 1B). This particular phosphodiester bond was also hydrolyzed by Pb^{2+}, Mn^{2+}, and Ca^{2+} ions (Figs. 1C, 2A). Exposure of 70S ribosomes to Ca^{2+} resulted in an unusual cleavage pattern in domain IV, characterized by a stretch of adjacent cuts between nt A1937 and G1945 (Figs. 1C, 2A). Three Ca^{2+} (U1834, U1982, U2022) and three Mn^{2+} (U1834, A1977, U2022) cuts were additionally mapped in domain IV (Fig. 2A).

The highly conserved domain V of the 23S rRNA, including the central loop, is generally considered to be the major element of the peptidyl transferase center of the ribosome. Three intermediate Pb^{2+} cleavages at positions C2347, C2440, and U2441 (Figs. 2A, 4A) and two weak cuts at C2573 and U2585 were identified. Mn^{2+} and Ca^{2+} ions also hydrolyzed the rRNA at C2347, C2440, and U2441 and at five additional sites in domain V (G2276, G2391, A2406, U2431, and A2432). One single Mn^{2+} cleavage in the central loop at G2502 was also observed (Fig. 2A). Mg^{2+} ions, which are the natural divalent metal ions in translating ribosomes in vivo, do not promote cleavage at any of the aforementioned positions, but target the RNA at C2385.

Domain VI of the 23S rRNA was specifically cleaved by Mg^{2+} ions at G2791, C2794, and G2801; the latter two positions are located within a proposed double helix. Ca^{2+} also promoted cleavage in this helix at C2793 and G2801, as well as in unpaired regions at G2791, U2833, and G2834. Mn^{2+} ions also induced hydrolysis at G2791 and G2834, whereas Pb^{2+} solely targeted position U2833 (Fig. 2A).

Metal ion cleavages in the 16S rRNA

Compared to the 23S rRNA, the 30S subunit was noticably less sensitive to specific cleavage directed by metal ions. Only 13 cleavage sites could be identified in the 16S rRNA, with the most pronounced situated in the 5′ domain at positions G240 and G245, at which all divalent cations tested hydrolyze the RNA (Figs. 1D, 2B). This position links two helices (the 260- and the 130/230-stem) that contribute to the recognition of the primary binding protein S17 (Powers & Noller, 1995) and is depicted at the bottom of the small subunit in 3D models of the 30S particle (Fink et al., 1996; Mueller & Brimacombe, 1997). In addition, two weak cleavage sites in the 5′ domain were mapped to G144 (Pb^{2+}, Mn^{2+}, and Ca^{2+}) and G211 (Pb^{2+} and Mn^{2+}) (Fig. 2B).

The central domain of the 16S rRNA was only cleaved by metal hydroxides at the three sites A532 by Pb^{2+}, A533 by Mn^{2+} and Ca^{2+}, and U562 by Mg^{2+} (Fig. 2B). A532 and A533 are located within the 530-loop, which can adopt a pseudoknot structure that requires that the rRNA be sharply bent (Masquida et al., 1991). Sensitivity of these two phosphodiester bonds to metal ion cleavage might result from this constraint.

The 3′ major domain was cut at nt G1182 and U1183 by Pb^{2+}, Mn^{2+}, and Ca^{2+} (Fig. 2B). These nucleotides are located in a region involved in binding of the secondary binding protein S9 (Powers & Noller, 1995), which is located in the head region of the small subunit (Mueller & Brimacombe, 1997). Another part of the S9 binding site is proposed to be created by the 1250/1280 region, arguing for a tertiary interaction of these two arms of the 3′ major domain. Consistent with this notion is that nucleotides sensitive to metal ion-catalyzed hydrolysis were also found in the 1250/1280 region (A1257 to Pb^{2+}, Mg^{2+}, Mn^{2+}, Ca^{2+}; G1258 to Mg^{2+}, Mn^{2+}, Ca^{2+}; and A1285 to Pb^{2+}) (Fig. 2B). This suggests that the proposed tertiary structure around S9 is one of the few parts of 16S rRNA that are accessible to cleaving divalent cations.

It is interesting to note that the entire 3′ minor domain, containing the decoding region, was not cleaved by metal ions at all under our conditions. This region has already been the target of lead cleavage experiments using 3′ end-labeled 16S rRNA (Gornicki et al., 1989). In these studies, most of the observed cleavages in the 3′ minor domain of naked 16S rRNA were not detected in 70S ribosomes, suggesting protection by ribosomal proteins or structural rearrangements of the rRNA in the RNP particle.

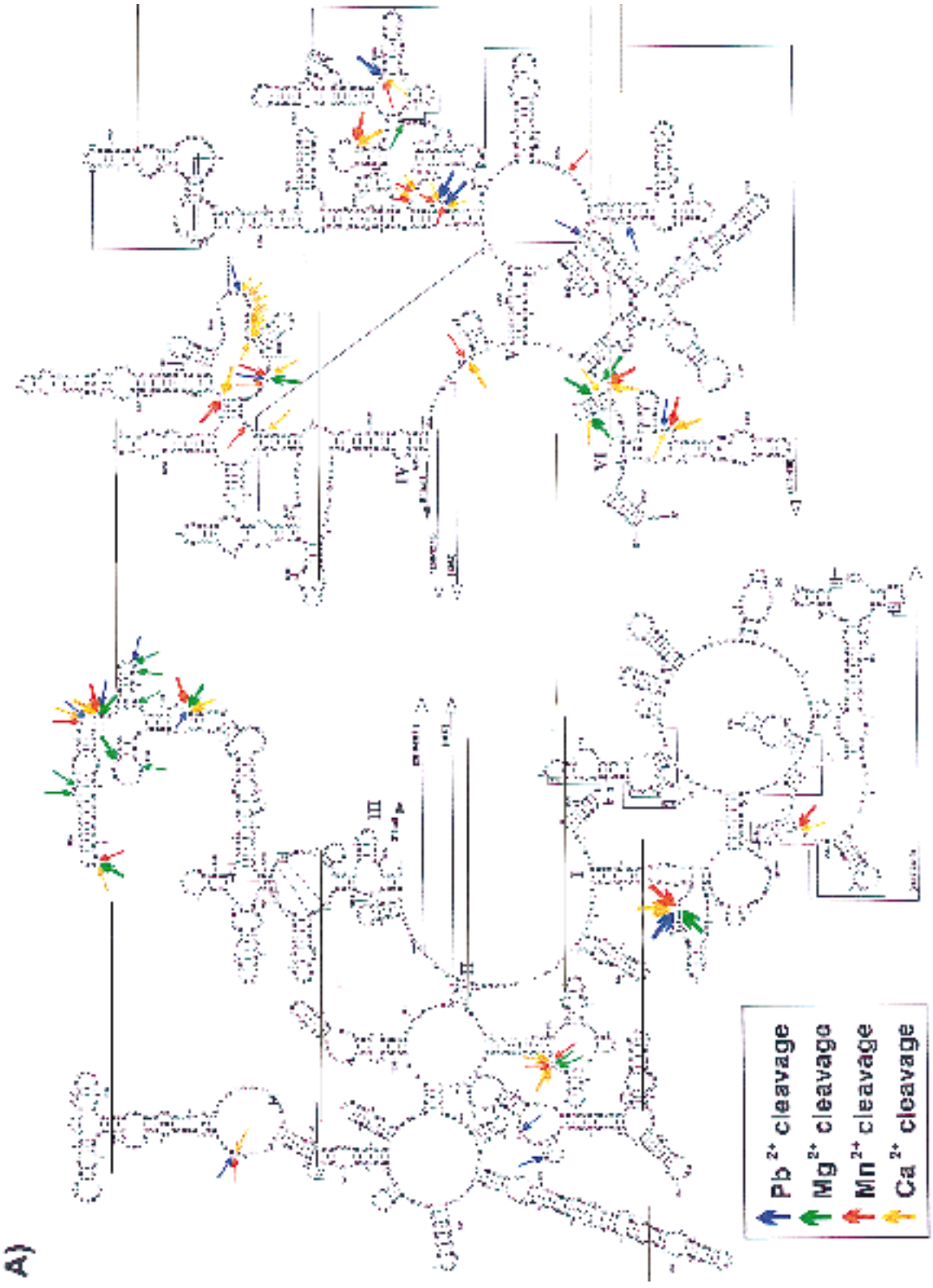

FIGURE 2. (*Figure continues on facing page.*)

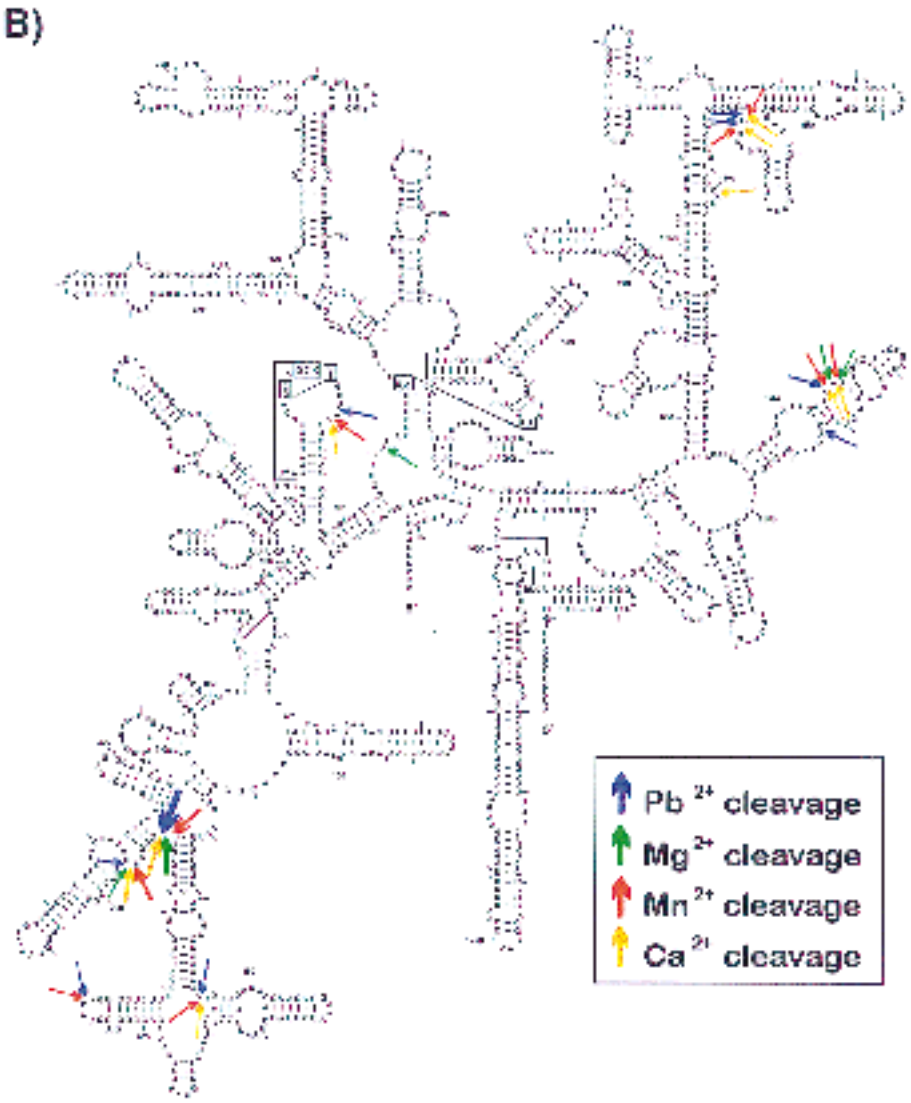

FIGURE 2. Summary of divalent metal ion cleavage sites in 23S rRNA (**A**) and 16S rRNA (**B**) of *E. coli*. Location of specific strand scissions in the secondary structure models (Gutell et al., 1994) catalyzed by Pb^{2+}, Mg^{2+}, Mn^{2+}, and Ca^{2+} are indicated by colored arrows (see color code) whereby the thickness of the arrows corresponds to the cleavage efficiency. Strong cleavages are shown by thick arrows, intermediate cleavages by medium arrows, and weak cleavages by thin arrows.

Influence on Pb^{2+} cleavage upon tRNA binding

Because some of the metal cleavage sites occur in regions implicated in tRNA binding, we investigated the effects of bound ligands on the specific Pb^{2+} hydrolysis in the peptidyl transferase center and in the 530-loop. To this end, we induced the cleavage reaction after tRNA or AcPhe-tRNA binding to the P site of poly(U) programmed ribosomes. Interestingly, binding of AcPhe-tRNA resulted in decreased lead cleavage efficiency at A1966 of domain IV of 23S rRNA. The relative cleavage rate was reduced about 30% upon AcPhe-tRNA binding, but was unaffected upon binding of uncharged tRNA (Fig. 3). For comparison, Pb^{2+} cleavage at A1937 (also located in domain IV), C2347, C2440, U2441, C2573, U2585 (all located in domain V), and at A532 (located in the 530-loop in 16S rRNA) were not affected by tRNA binding at all (data not shown).

Are metal ion binding sites conserved in evolution?

Because metal cleavage sites are strictly determined by the positioning of the attacking metal hydroxide, an identical cleavage pattern is a consequence of a similar binding mode of the metal ion and hence of a conserved tertiary RNA structure. Parts of the secondary structure of rRNAs are highly conserved, particularly in regions implicated in building the active sites. However, little is known about their three-dimensional shapes. In order to gain insight into a possible generality of the

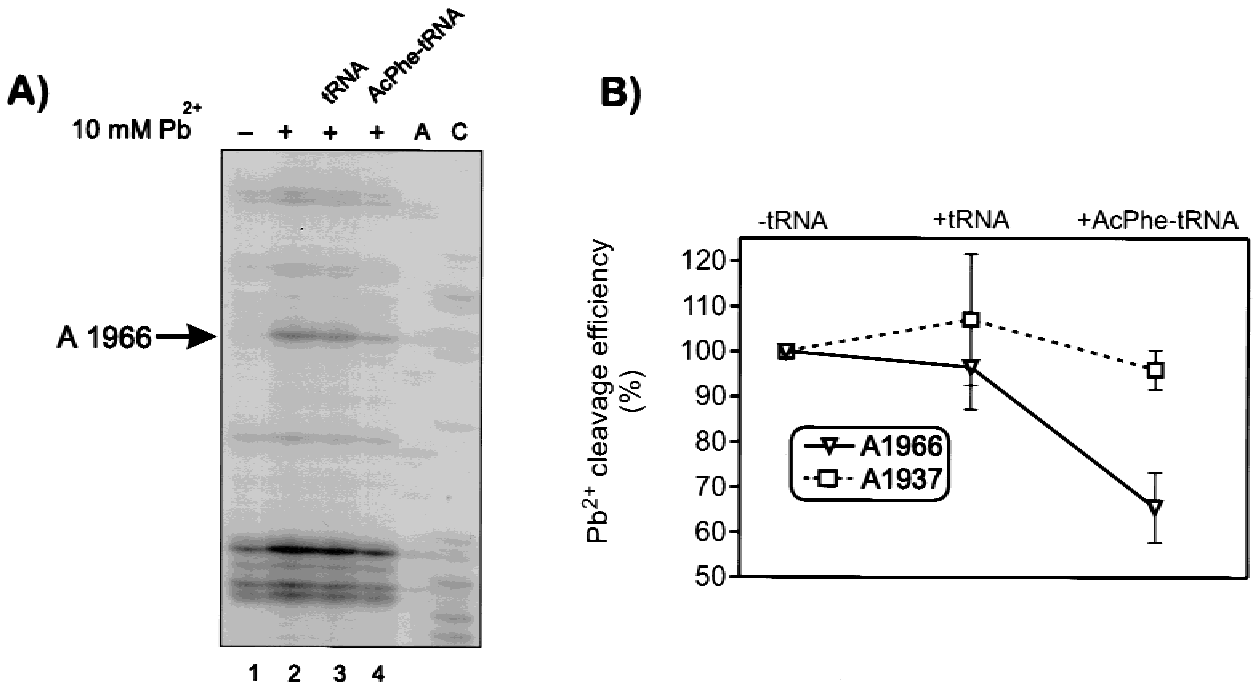

FIGURE 3. Effect of tRNA binding on two Pb^{2+} cleavage sites in domain IV of 23S rRNA. **A:** Influence on Pb^{2+} cleavage at A1966 upon binding of tRNAs. Lane 1 shows the reverse transcription of uncleaved poly(U) programmed ribosomes. The cleavage reaction was performed with 10 mM $Pb(OAc)_2$ in the absence of tRNA (lane 2) and in the presence of P site-bound uncharged tRNA (lane 3) or AcPhe-tRNA (lane 4). AC denote sequencing lanes. **B:** Effects of bound AcPhe-tRNA and uncharged tRNA to the P site were quantified by using a Molecular Dynamics PhosphorImager. The lead-cleavage efficiency of poly(U) programmed ribosomes at 10 mM $Pb(OAc)_2$ was taken as 100%. Quantification was performed for six independent binding experiments.

metal cleavage sites in the rRNAs, we compared the Pb^{2+}-cleavage patterns of *E. coli* and *Homo sapiens* ribosomes. Indeed, the highly conserved domain V of 23S-like rRNAs was hydrolyzed by Pb^{2+} ions at exactly homologous positions (C2347 and C2440, *E. coli* nomenclature), thus providing strong evidence for a very similar architecture of the rRNA at the peptidyl transferase center (Figs. 4A, 5A). These data not only confirm that metal ion binding pockets in domain V are highly conserved between two phylogenetically distant organisms, but also show that the RNA-cleaving nucleophiles, the lead hydroxide ions, are coordinated in identical orientations. Additionally, in domain I of the 23S-like rRNAs, Pb^{2+} ions also induced strand scission at a structurally homologous site at position A505 (*E. coli* nomenclature), which is situated in a conserved part of the domain (Figs. 4B, 5B). One cleavage site at G1197 (*H. sapiens* nomenclature) of domain I was identified in a region of the 28S rRNA that is missing in *E. coli* and many other organisms.

In contrast, although the human 18S rRNA was cut very efficiently by Pb^{2+} in its 5′ domain as in *E. coli* ribosomes, the positions did not correspond (Figs. 4C, 5C). Strand scission was mapped to C369 and G370, which are located 3′ of the *E. coli* cleavage site at G240 (*E. coli* nomenclature) in the 260-stem (Fig. 5C). These findings suggest that the 5′ parts of the 16S-like rRNAs fold slightly differently.

DISCUSSION

Metal ion hydroxide-catalyzed specific cleavage of rRNAs was applied to the characterization of the immediate environment of high-affinity cation binding pockets and to probe the fine structure of rRNAs within the active ribosome. For the maintainance of the structural as well as the functional integrity, ribosomes strictly require counterions, such as polyamines, mono-, and divalent metal ions. Whereas polycations and monovalent ions are interchangeable, divalent metal ions are required absolutely and cannot be substituted without destroying the catalytic activity (for a review, see Streicher & Wallis, 1996).

Metal ion-directed cleavage using Pb^{2+}, as well as the functionally active ions Mg^{2+}, Mn^{2+}, and Ca^{2+}, resulted in the identification of specific cleavage sites with various efficiencies. Site-specific and strong metal hydroxide cuts are caused by ions bound tightly to binding pockets in close physical proximity to the cleavage site and depend on a correct tertiary RNA folding. In contrast, metal ion cleavage can also be applied to probe the overall structure of RNA molecules. In this

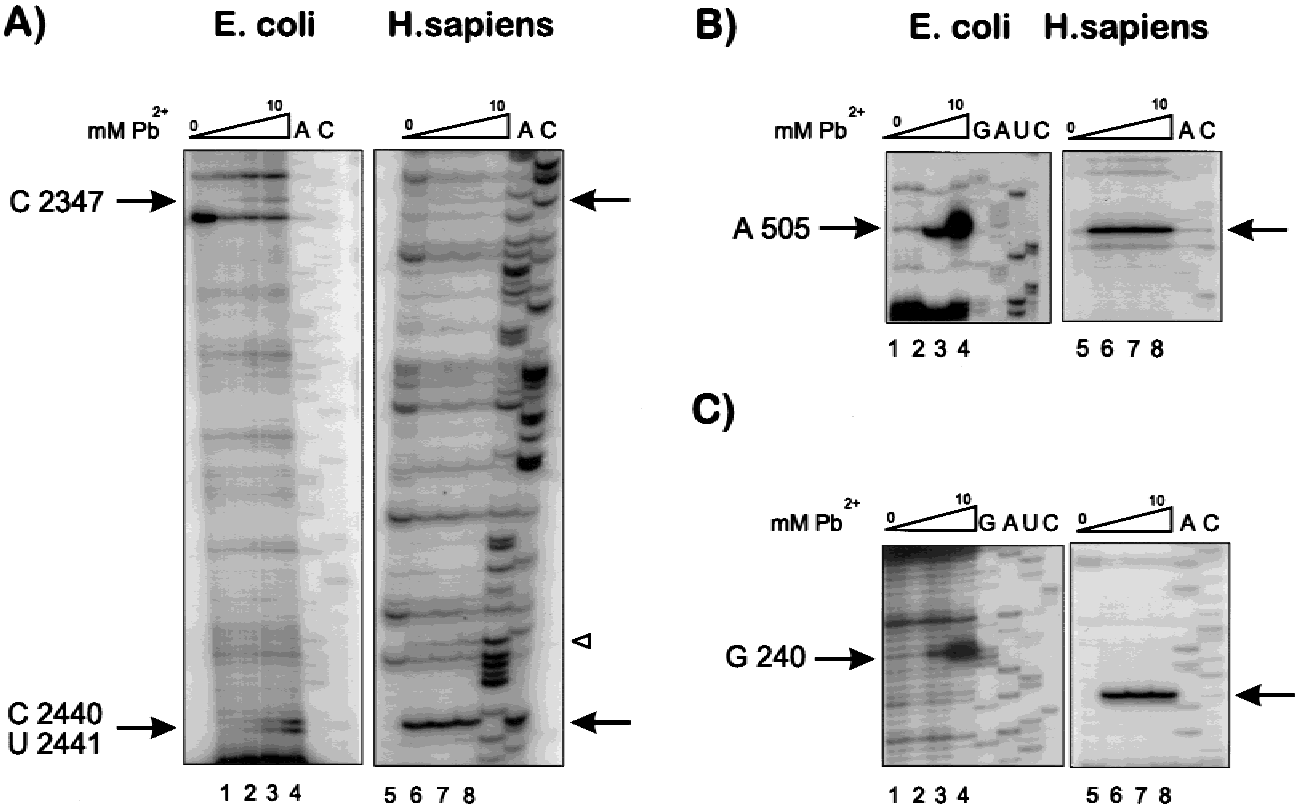

FIGURE 4. Comparison of the Pb^{2+} cleavage patterns of *E. coli* and *H. sapiens* ribosomes. Pb^{2+} concentrations for initiating the reaction in *E. coli* ribosomes were 0, 6, 8, or 10 mM (**A:** lanes 1–4) or 0, 3, 5, or 10 mM (**B,C:** lanes 1–4) and was performed for 4 min. Cleavage of HeLa cell ribosomes was initiated by the addition of 0, 3, 5, or 10 mM $Pb(OAc)_2$ (lanes 5–8) and was performed at 37 °C for 10 min. AC and GAUC indicate dideoxy sequencing lanes. Primer extension of domain V of 23S-like rRNA (A), domain I of 23S-like rRNA (B), and of the 5′ domain of 16S-like rRNA (C) are shown. Open arrowhead in A marks a Pb^{2+} cleavage at A4336 in 80S ribosomes.

case, the metal ions act from the solution and preferentially cleave every acessible single-stranded nucleotide with low efficiency and slow cleavage rate; this is sometimes termed “unspecific cleavage” (Pan et al., 1993).

Site-specific metal hydroxide-induced cleavage is considered to occur in single-stranded and flexible regions, whereas double-stranded RNA helices are known to be insensitive (Gornicki et al., 1989; Ciesiolka et al., 1998). In fact, apart from two exceptions, all characterized cleavage sites are located in single strands and in unpaired parts of typical RNA secondary structure elements like bulges (23S rRNA: 1510, 1982, 2440, 2573; 16S rRNA: 1201), internal loops (23S rRNA: 1026, 1523, 1555; 16S rRNA: 1257, 1285), hairpins (23S rRNA: 785, 1452, 1461, 1494, 1537, 2276; 16S rRNA: 211, 532), three-way junctions (23S rRNA: 792, 2833), four-way junctions (23S rRNA 653, 1544, 1977, 2347; 16S rRNA: 144, 240), or in multi-branched loops (23S rRNA: 1834, 1966, 2022, 2502, 2585). In the first exception, Ca^{2+}-promoted cleavage resulted in hydrolysis of adjacent phosphodiester bonds from positions A1937 to G1945 in domain IV of the 23S rRNA (Figs. 1C, 2A). This interesting cleavage pattern significantly was seen only with Ca^{2+} and Eu^{3+} ions (S. Dorner, unpubl.); these ions share a common ion radius, but have different pK_a values (12.6 for Ca^{2+} and 8.6 for Eu^{3+}). Because the same cleavage pattern was obtained at neutral pH with Eu^{3+} (and to a lesser extent with Pb^{2+}; data not shown), a pH effect can be ruled out. Therefore, it can be concluded that the native structure was probed in all cases. In some 2D models (Noller et al., 1981; Brimacombe & Stiege, 1985), this region is involved in forming a helix, which should make it resistant to metal ion cleavage. In light of our data, this region is not supposed to be base paired, a conclusion that is supported further by data showing nucleotides in that region to be highly reactive to single-strand-specific chemical probes (Egebjerg et al., 1990) and by a structure model that depicts this region unpaired (Fig. 2A). Second, two Mg^{2+} (C2794 and G2801) and two Ca^{2+} cuts (C2793 and G2801) in domain VI of 23S rRNA could be identified (Fig. 2A) that are located within a helical region. Comparative sequence analysis suggests a canonical base paired helix; however, this helix apparently adopts a structure that is accessible to site-specific cleavage, at least under the Mg^{2+} and

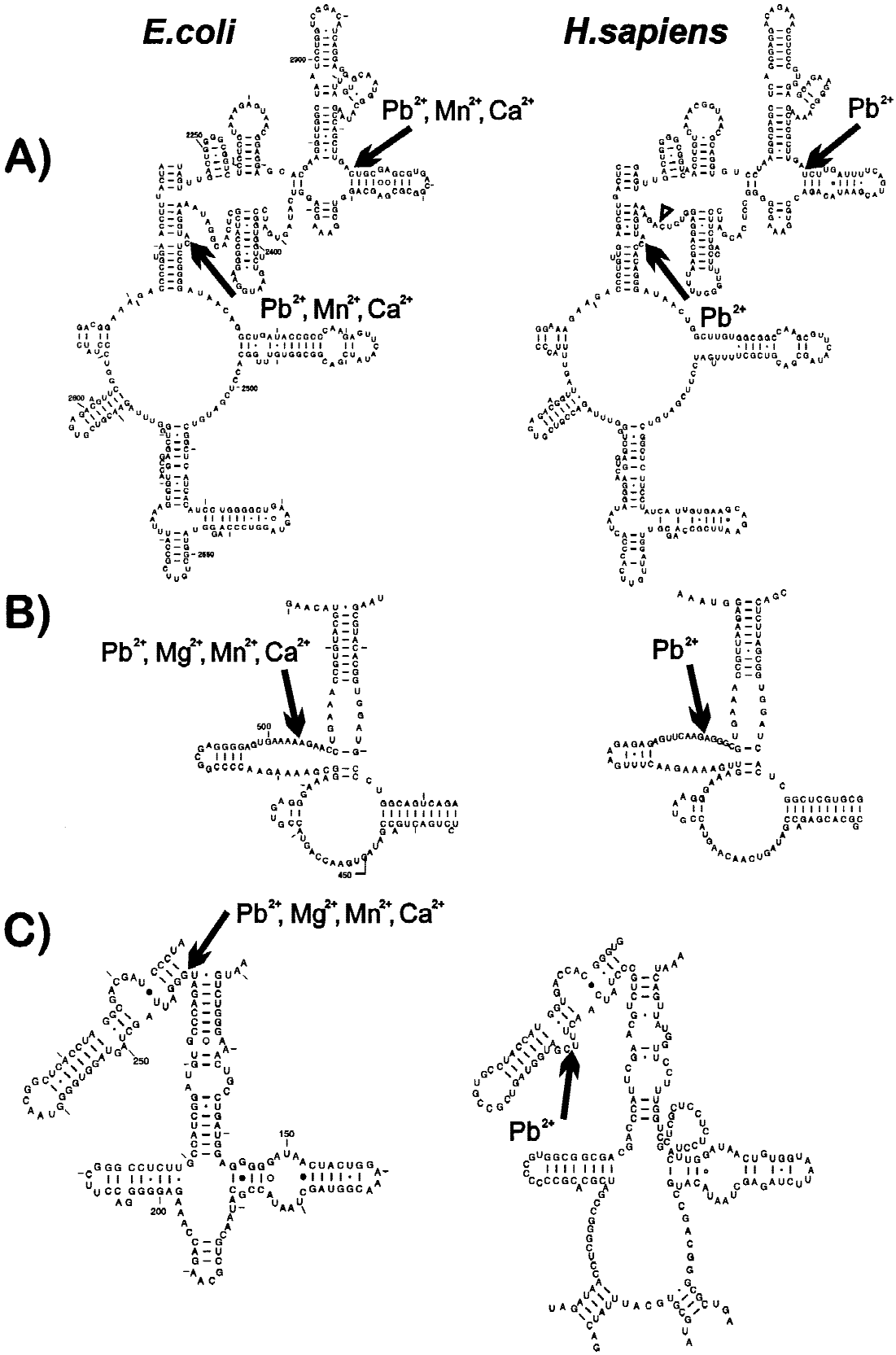

FIGURE 5. Comparison of the location of metal ion cleavage sites identified in *E. coli* and *H. sapiens* rRNAs. Sites of strand scission in the secondary structure models of *E. coli* (left) and *H. sapiens* (right) rRNAs are indicated by arrows. **A:** Domain V of 23S-like rRNA. **B:** Domain I of 23S-like rRNA. **C:** 5′ Domain of 16S-like rRNA. The open arrowhead in A marks a cleavage at A4336 in 80S ribosomes.

Ca^{2+} cleavage conditions (elevated pH and higher temperatures).

Hairpins, being the most abundant elements of RNA secondary structure (Woese et al., 1990), are thought to provide nucleation points for folding and are often involved in protein recognition (Varani, 1995). In rRNAs, the most frequent hairpins contain the so called tetraloops of the GNRA, UNCG, and CUUG families. The four nucleotides in the loops are structurally constrained, which explains the unusual thermodynamic stability of the hairpin. The 70S ribosomal tetraloops were resistant to metal ion cleavage, with only two exceptions. Two UNCG tetraloops, located in domain III of the 23S rRNA (U1534–G1537) (Fig. 2A) and in the 5′ domain of 16S rRNA (U208–G211) (Fig. 2B), were cut by Pb^{2+} and Mg^{2+}, or Pb^{2+} and Mn^{2+}, respectively. In each case, the cleavage was mapped to the guanosine closing the loop, known to be the only base in *syn*-conformation that results in an unusual backbone conformation at that residue (Varani, 1995). Because tetraloops are often involved in long-range interactions (Costa & Michel, 1995), a possible explanation is that these two tetraloops are not involved in tertiary interactions or protein binding, thus making them accessible for cleavage.

Highly efficient divalent metal ion cleavage sites in RNA are indicative of structurally adjacent cation binding pockets. Two phosphodiester bonds in *E. coli* ribosomes at positions A505 in domain I of the 23S rRNA (Figs. 1A, 2A) and G240 of the 5′ domain of 16S rRNA (Figs. 1D, 2B) were cleaved efficiently and specifically by Pb^{2+}, Mg^{2+}, Mn^{2+}, and Ca^{2+}. In a previous paper, we could demonstrate that Pb^{2+} cleavage at these sites can be inhibited by increasing amounts of Mg^{2+}, Mn^{2+}, and Ca^{2+}, thus arguing strongly for overlapping binding sites (Winter et al., 1997). Here we present evidence that these metal hydroxides fit into the same binding pocket and are positioned in a way to initiate site-specific hydrolysis of a particular phosphodiester bond. Both strong sites of cleavage are located near the 5′ ends of 23S and 16S rRNA, respectively, regions that fold into highly structured and stable domains even in the absence of ribosomal proteins (Branlant et al., 1981; Stiegler et al., 1981; Powers & Noller, 1995). In support of this, the strong Pb^{2+} cleavages at A505 in domain I of 23S rRNA and at G240 in the 5′ domain of 16S rRNA could still be detected in phenolized ribosomes (Winter, 1994 and data not shown), providing further evidence for a role of metal ions in supporting tertiary structure of these rRNA domains. Indeed, addition of the primary binding protein L24, which binds at sites including the conserved region around A505, resulted in only minor changes of the chemical reactivities of nucleotides in this region (Egebjerg et al., 1987). All these data led us to consider that metal ion-coordinated structure is the primary cause for the architecture of the 5′ parts of 23S and 16S rRNA. This appears to be analogous to a recently characterized magnesium ion core in a ribozyme domain that drives the hierarchical folding pathway (Cate et al., 1997).

A region of more functional interest is built by domain IV and V of the 23S rRNA. The strong conservation as well as the accumulation of tRNA footprint- (Moazed & Noller, 1989), tRNA crosslink- (Steiner et al., 1988; Wower et al., 1989; Mitchell et al., 1993), and antibiotic interaction sites (Noller, 1984; Sor & Fukuhara, 1984; Douthwaite et al., 1985; Ettayebi et al., 1985; Moazed & Noller, 1987) in substantial parts of domain IV and V (Fig. 6) argue strongly for a direct involvement of this region in tRNA binding and in catalyzing peptide bond formation. The most efficient metal ion cleavage sites in the peptidyl transferase center were mapped to positions C2347, C2440, and U2441, at which Pb^{2+}, Mn^{2+}, and Ca^{2+} induced strand scission (Figs. 2A, 4A). The latter two positions are located in a two-nucleotide bulge that is considered to be very close to the active center. This notion is strengthened by the finding that A or P site-bound Phe-tRNA protects position A2439 from chemical modification (Moazed & Noller, 1989) and by crosslinking data of P site-bound Phe-tRNA to the same nucleotide (Mitchell et al., 1993). Interestingly, Mg^{2+} ions did not cut domain V of the rRNA at the aforementioned positions, but cleave at a single site at C2385. Because Pb^{2+} cleavage at C2347, C2440, and U2441 (Winter et al., 1997 and data not shown) could be inhibited in competition experiments using increasing amounts of Mg^{2+}, we concluded that Mg^{2+} binds to the same general metal binding site(s) from which Pb^{2+}, Mn^{2+}, and Ca^{2+} attacked C2347, C2440, and U2441, but with a different coordination.

The most efficient general cleavage site in domain IV was identified 5′ to A1966 (Fig. 2A). Binding of AcPhe-tRNA to the P site resulted in a decrease in Pb^{2+} cleavage efficiency at this site; however, cleavage was not affected by binding of uncharged tRNA (Fig. 3). The observed inhibitory effect could be either due to a structural change of this part of domain IV upon AcPhe-tRNA binding, or due to shielding of A1966 because of a close physical proximity of this site to the amino acid moiety of charged tRNAs. The latter is in close agreement with hydroxyl radical probing approaches with Fe(II) attached via an EDTA linker to the 5′ end of A or P site-bound tRNA that resulted in cleavages in the 1940–1970 region of domain IV (Joseph & Noller, 1996).

Other cleavages that are located in the peptidyl transferase center (C2347, C2440, U2441, C2573, U2585) or in the 530-loop of 16S rRNA (A532) were not affected by tRNA binding. This indicates that these positions were cleaved by metal ions that were bound to binding sites that do not overlap with tRNA binding sites or to pockets that are not disturbed upon tRNA binding.

In conclusion, divalent metal ions creating strand scission at positions A1966, C2347, C2440, and U2441 are

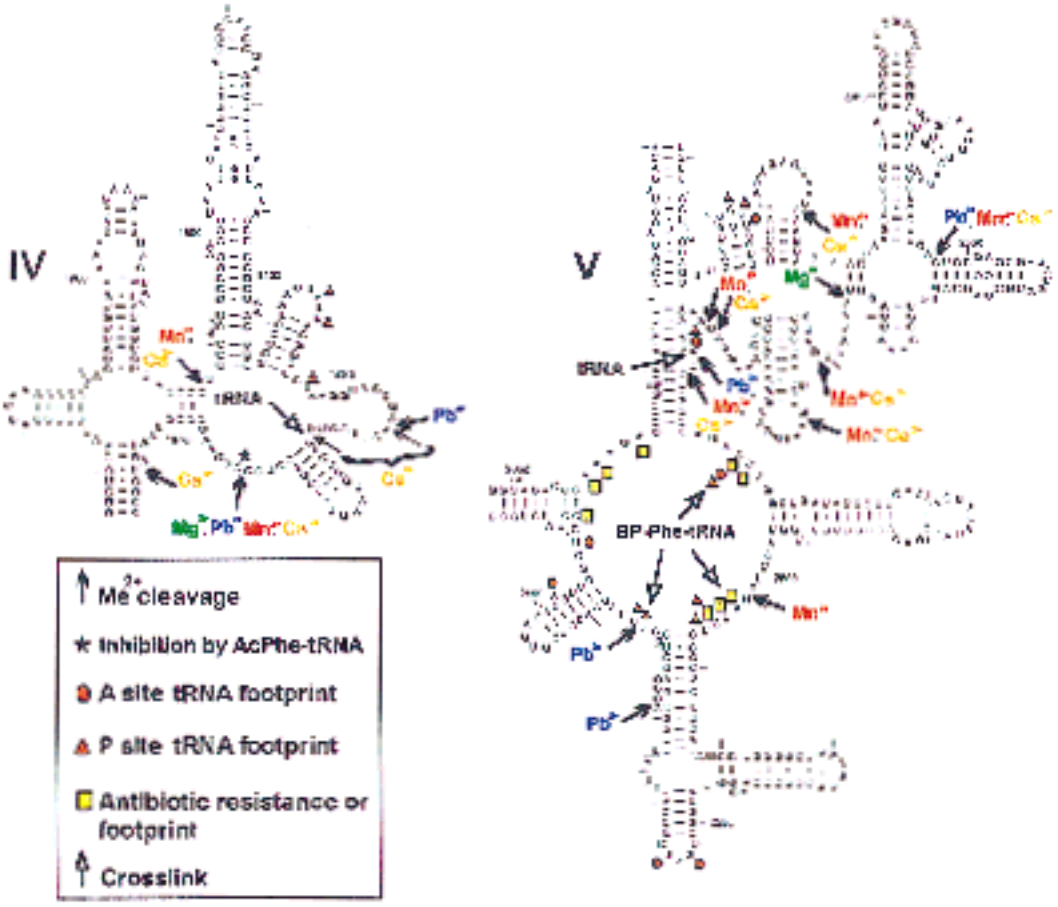

FIGURE 6. Metal ion cleavage sites in the peptidyl transferase center of *E. coli*. Location of the cleavage sites in domain IV (left) and V (right) of 23S rRNA are indicated by filled arrows. Nucleotides that are protected from chemical modification by A site- (circle) or P site-bound tRNA (triangle) are also shown (Moazed & Noller, 1989). Sites of crosslinking of derivatives of tRNA are indicated by open arrows (Steiner et al., 1988; Wower et al., 1989; Mitchell et al., 1993). Squares indicate nucleotides at which mutation confers resistance to peptidyl transferase-directed antibiotics (Noller, 1984; Sor & Fukuhara, 1984; Douthwaite et al., 1985; Ettayebi et al., 1985) or bases that show an alteration of reactivity toward chemical modification upon antibiotic binding (Moazed & Noller, 1987). Asteriks mark the position where P site-bound AcPhe-tRNA resulted in reduced Pb^{2+} cleavage efficiency.

considered to act from binding sites located close to the peptidyl transferase center. These metal ions are of particular interest because it has been proposed recently that peptide bond formation might be metal ion-catalyzed (Barta & Halama, 1996; Winter et al., 1997). One prediction from this assumption is that metal ion binding pockets should be as evolutionarily conserved as peptide bond formation and hence the architecture of the peptidyl transferase active site should be very similar.

We therefore applied metal ion cleavage of rRNAs from two phylogenetically distant organisms (*E. coli* and *H. sapiens*) to compare the metal ion cleavage patterns with regard to phylogenetic conservation. Metal ion-directed cleavage is a very sensitive method to monitor the fine structure of RNA and has been applied widely (Gornicki et al., 1989; Kazakov & Altman, 1991; Zito et al., 1993; Ciesiolka et al., 1998). In some cases, Pb^{2+}-induced cleavage was even more sensitive to monitor faint structural differences in tRNA variants than nuclease digestion (Michalowski et al., 1996).

The cleavage pattern exhibited by the 5′ domain of human 18S rRNA is distinct from that of *E. coli* (Fig. 5C). This region of the 16S-like rRNAs is not so highly conserved in primary sequence, but shows similarities in secondary structure. The fact that the Pb^{2+} cleavage pattern of the 5′ domain was clearly distinguishable between 70S and 80S ribosomes suggests that similar secondary structure models do not necessarily indicate identical tertiary folding of RNA domains. In contrast, the identification of three Pb^{2+} cleavage sites at exactly homologous positions in the 23S-like rRNA of *E. coli* and *H. sapiens* led us to conclude that the tertiary structures around positions A505 in domain I and C2347 and C2440 in domain V of the peptidyl transferase center are very similar and therefore highly conserved throughout evolution (Fig. 5A,B). It is further evident that these conserved rRNA tertiary structures are capable of binding

divalent cations in specific binding pockets. These findings indicate that strictly coordinated divalent metal ions, fitting into phylogenetically highly conserved binding centers, might fulfill essential roles in ribosomes.

Our data not only argue for an identical positioning of metal ions in the catalytic heart of eubacterial and human ribosomes, but also indicate that tight metal ion binding pockets are located in close physical proximity to the active site of peptide bond formation in all ribosomes. In conclusion, the data presented in this paper support further our earlier proposal (Barta & Halama, 1996; Winter et al., 1997) that peptidyl transfer might be a metal ion-catalyzed process, for which phylogenetically conserved cation binding pockets near the active center are a prerequisite.

MATERIALS AND METHODS

Ribosomes and tRNAs

Ac[^{3}H]Phe-tRNA and 70S ribosomes (from *E. coli* strain D10) were prepared as described (Rheinberger et al., 1988). MRE-600 ribosomes were kindly provided by M. Rodnina and W. Wintermeyer (Rodnina & Wintermeyer, 1995).

Metal ion cleavage procedure

Pb^{2+} cleavage was performed in buffer A (20 mM Tris/Cl, pH 7.5, 6 mM $MgCl_2$, 100 mM KCl, 0.4 mM EDTA, 2 mM DTT) as described (Winter et al., 1997). A typical 20-μL Mg^{2+} cleavage reaction contained 12 pmol ribosomes in buffer B (20 mM Glycin/NaOH, pH 9, 10 mM $MgCl_2$, 100 mM KCl, 0.4 mM EDTA, 2 mM DTT) and was performed at 45 °C for the indicated period of time. For the Mn^{2+} and Ca^{2+} cleavage, Mg^{2+} ions (originating from the ribosome storage buffer) were substituted by passing the ribosomes over a gel filtration column (Sephacryl S-300; cDNA spun column; Pharmacia) and eluted with buffer C or D, respectively (buffer C: 20 mM Tris/Cl, pH 8, 2–15 mM $MnCl_2$, 100 mM KCl, 0.4 mM EDTA, 2 mM DTT; buffer D: 20 mM Glycin/NaOH, pH 9, 2–15 mM $CaCl_2$, 100 mM KCl, 0.4 mM EDTA, 2 mM DTT). A 50-μL Mn^{2+} or Ca^{2+} cleavage reaction contained 25 pmol ribosomes and was performed at 45 °C for the time indicated in the figures.

Human 80S ribosomes were prepared by centrifugation of 200-μL HeLa-cell extract (S20), prepared as described (Liebig et al., 1993), for 45 min at 100,000 $\times$ *g*. The ribosome pellet was resuspended in 60 μL buffer A and the Pb^{2+} cleavage was performed by preincubating 2 μL ribosome solution in 20 μL buffer A for 15 min at room temperature followed by addition of $Pb(OAc)_2$ to a final concentration ranging from 3 to 10 mM and was performed for 10 min at 37 °C. All cleavage reactions were stopped and the rRNAs were purified as described previously (Winter et al., 1997).

Binding of tRNA

Ten picomoles 70S ribosomes were incubated with 10 μg poly(U) in 30 μL buffer A for 10 min at 37 °C. Ten picomoles tRNA or Ac[^{3}H]Phe-tRNA in 20 μL of the same buffer were added and incubated for 20 min at 37 °C and held on ice for 20 min. Pb^{2+} cleavage was initiated afterward by addition of $Pb(OAc)_2$ to a final concentration of 10 mM and performed as mentioned above.

Reverse transcriptase analysis

About 1 pmol rRNA was used as template for primer extension and was hybridized to 0.3–0.6 pmol ^{32}P-end labeled oligonucleotides. The primers for 23S and 16S rRNA were as in Winter et al. (1997). Primers were complementary to nt 451–467, 1295–1311, 1498–1514, 3857–3873, and 4400–4416 for human 28S rRNA and to nt 444–460 and 676–692 for 18S rRNA. Primer extension was performed in a buffer containing 122.5 mM Tris/Cl, pH 8.4, 11 mM $MgCl_2$, 15 mM KCl, 11 mM DTT, 0.25 mM dNTPs with 0.4 units AMV reverse transcriptase (Life Science) for 45 min at 42 °C. For sequencing reactions, dideoxynucleotides were added to a concentration of 7 μM. cDNA products were ethanol precipitated and separated on 6% polyacrylamide gels. Quantitative data were obtained by using a Molecular Dynamics PhosphorImager.

ACKNOWLEDGMENTS

We are grateful to Tim Skern and Iris Hoch for critical review of the manuscript; to Isabella Halama for valuable comments; and to Wolfgang Wintermeyer for the gift of MRE-600 ribosomes. Our thanks are extended to Renee Schroeder and Harry Noller for fruitful discussions and to all participants of the "Z. Raxler-Memorial-Recess '97." This work was supported by grants (P09454-MIB and P12195-GEN) from the Österreichischer Fonds zur Förderung der wissenschaftlichen Forschung to A.B.

Received February 27, 1998; returned for revision March 26, 1998; revised manuscript received June 23, 1998

REFERENCES

Allain FHT, Varani G. 1995. Divalent metal ion binding to a conserved wobble pair defining the upstream site of cleavage of group I self-splicing introns. *Nucleic Acids Res 23*:341–350.

Baeyens KJ, De Bondt HL, Pardi A, Holbrook S. 1996. A curved RNA helix incorporating an internal loop with G A and A A non-Watson–Crick base pairing. *Proc Natl Acad Sci USA 93*:12851–12855.

Barta A, Halama I. 1996. The elusive peptidyltransferase–RNA or protein? In: Green R, Schroeder R, eds. *Ribosomal RNA and group I introns*. New York: R.G. Landes Company/Chapman & Hall. pp 35–54.

Branlant C, Krol A, Machatt MA, Pouyet J, Ebel JP, Edwards K, Kossel H. 1981. Primary and secondary structures of *Escherichia coli* MRE 600 23S ribosomal RNA. Comparison with models of secondary structure for maize chloroplast 23S rRNA and for large portions of mouse and human 16S mitochondrial rRNAs. *Nucleic Acids Res 9*:4303–4324.

Brimacombe R, Stiege W. 1985. Structure and function of ribosomal RNA. *Biochem J 229*:1–17.

Brown RS, Dewan JC, Klug A. 1985. Crystallographic and biochemical investigation of the lead(II)-catalyzed hydrolysis of yeast phenylalanine tRNA. *Biochemistry 24*:4785–4801.

Brown RS, Hingerty BE, Dewan JC, Klug A. 1983. Pb(II)-catalysed cleavage of the sugar-phosphate backbone of yeast tRNAPhe—Implications for lead toxicity and self-splicing RNA. *Nature 303*:543–546.

Cate JH, Doudna JA. 1996. Metal-binding sites in the major groove of a large ribozyme domain. *Structure 4*:1221–1229.

Cate JH, Hanna L, Doudna JA. 1997. A magnesium ion core at the heart of a ribozyme domain. *Nature Struct Biol 4*:553–558.

Ciesiolka J, Michalowski D, Wrzesinski J, Krajewski J, Krzyzosiak WJ. 1998. Patterns of cleavages induced by lead ions in defined RNA secondary structure motifs. *J Mol Biol 275*:211–220.
Correll CC, Freeborn B, Moore PB, Steitz TA. 1997. Metals, motifs, and recognition in the crystal structure of a 5S rRNA domain. *Cell 91*:705–712.
Costa M, Michel F. 1995. Frequent use of the same tertiary motif by self-folding RNAs. *EMBO J 14*:1276–1285.
Douthwaite S, Prince JB, Noller HF. 1985. Evidence for functional interaction between domains II and V of 23S ribosomal RNA from an erythromycin-resistant mutant. *Proc Natl Acad Sci USA 82*:8330–8334.
Egebjerg J, Larsen N, Garret RA. 1990. Structural map of 23S rRNA. In: Dahlberg A, Garrett RA, Moore PB, Schlessinger D, Warner JR, eds. *The ribosome: Structure, function and evolution*. Washington, DC: ASM. pp 168–179.
Egebjerg J, Leffers H, Christensen A, Andersen H, Garrett RA. 1987. Structure and accessibility of domain I of *Escherichia coli* 23 S RNA in free RNA, in the L24-RNA complex and in 50 S subunits. Implications for ribosomal assembly. *J Mol Biol 196*:125–136.
Ettayebi M, Prasad SM, Morgan EA. 1985. Chloramphenicol-erythromycin resistance mutations in a 23S rRNA gene of *Escherichia coli*. *J Bacteriol 162*:551–557.
Fink DL, Chen RO, Noller HF, Altman RB. 1996. Computational methods for defining the allowed conformational space of 16S rRNA based on chemical footprinting data. *RNA 2*:851–866.
Gautheret D, Konings D, Gutell RR. 1994. A major family of motifs involving G.A mismatches in ribosomal RNA. *J Mol Biol 242*:1–8.
Gautheret D, Konings D, Gutell RR. 1995. G U base pairing motifs in ribosomal RNA. *RNA 1*:807–814.
Gornicki P, Baudin F, Romby P, Wiewiorowski M, Kryzosiak W, Ebel JP, Ehresmann C, Ehresmann B. 1989. Use of lead(II) to probe the structure of large RNA's. Conformation of the 3′ terminal domain of *E. coli* 16S rRNA and its involvement in building the tRNA binding sites. *J Biomol Struct Dyn 6*:971–984.
Gutell RR, Larsen N, Woese CR. 1994. Lessons from an evolving rRNA: 16S and 23S rRNA structures from a comparative perspective. *Microbiol Rev 58*:10–26.
Joseph S, Noller HF. 1996. Mapping the rRNA neighborhood of the acceptor end of tRNA in the ribosome. *EMBO J 15*:910–916.
Kazakov S, Altman S. 1991. Site-specific cleavage by metal ion cofactors and inhibition of M1 RNA, the catalytic subunit of RNase P from *Escherichia coli*. *Proc Natl Acad Sci USA 88*:9193–9197.
Laing LG, Gluick TC, Draper DE. 1994. Stabilization of RNA structure by Mg ions. *J Mol Biol 237*:577–587.
Liebig HD, Ziegler E, Yan R, Hartmuth K, Klump H, Kowalski H, Blaas D, Sommergruber W, Frasel L, Lamphear B, Rhoads R, Kuechler E, Skern T. 1993. Purification of two picornaviral 2A proteinases: Interaction with eIF-4 gamma and influence on in vitro translation. *Biochemistry 32*:7581–7588.
Maden BEH, Monro RE. 1968. Ribosome-catalyzed peptidyl transfer. Effects of cations and pH value. *Eur J Biochem 6*:309–316.
Masquida B, Felden B, Westhof E. 1997. Context dependent RNA–RNA recognition in a three-dimensional model of the 16S rRNA core. *Bioorg Med Chem 5*:1021–1035.
Michalowski D, Wrzesinski J, Wlodzimierz K. 1996. Cleavages induced by different metal ions in yeast tRNAPhe U59C60 mutants. *Biochemistry 35*:10727–10734.
Mitchell P, Stade K, Osswald M, Brimacombe R. 1993. Site-directed cross-linking studies on the *E. coli* tRNA–ribosome complex: Determination of sites labelled with an aromatic azide attached to the variable loop or aminoacyl group of tRNA. *Nucleic Acids Res 21*:887–896.
Moazed D, Noller HF. 1987. Chloramphenicol, erythromycin, carbomycin and vernamycin B protect overlapping sites in the peptidyl transferase region of 23S ribosomal RNA. *Biochimie 69*:879–884.
Moazed D, Noller HF. 1989. Interaction of tRNA with 23S rRNA in the ribosomal A, P, and E sites. *Cell 57*:585–597.
Mueller F, Brimacombe R. 1997. A new model for the three-dimensional folding of *Escherichia coli* 16 S ribosomal RNA. II. The RNA–protein interaction data. *J Mol Biol 271*:545–565.
Nitta I, Ueda T, Watanabe K. 1998. Possible involvement of *Escherichia coli* 23S ribosomal RNA in peptide bond formation. *RNA 4*:257–267.
Noller HF. 1984. Structure of ribosomal RNA. *Annu Rev Biochem 53*:119–162.
Noller HF, Hoffarth V, Zimniak L. 1992. Unusual resistance of peptidyl transferase to protein extraction procedures. *Science 256*:1416–1419.
Noller HF, Kop J, Wheaton V, Brosius J, Gutell RR, Kopylov AM, Dohme F, Herr W, Stahl DA, Gupta R, Woese CR. 1981. Secondary structure model for 23S ribosomal RNA. *Nucleic Acids Res 9*:6167–6189.
Pan T, Dichtl B, Uhlenbeck OC. 1994. Properties of an in vitro selected Pb2+ cleavage motif. *Biochemistry 33*:9561–9565.
Pan T, Long DM, Uhlenbeck OC. 1993. Divalent metal ions in RNA folding and catalysis. In: Gesteland RF, Atkins JF, eds. *The RNA world*. Cold Spring Harbor, New York: Cold Spring Harbor Laboratory Press. pp 271–302.
Pestka S. 1972. Peptidyl-puromycin synthesis on polysomes from *Escherichia coli*. *Proc Natl Acad Sci USA 69*:624–628.
Pley HW, Flaherty KM, McKay DB. 1994. Three-dimensional structure of a hammerhead ribozyme. *Nature 372*:68–74.
Powers T, Noller HF. 1995. Hydroxyl radical footprinting of ribosomal proteins on 16S rRNA. *RNA 1*:194–209.
Rheinberger HJ, Geigenmuller U, Wedde M, Nierhaus KH. 1988. Parameters for the preparation of *Escherichia coli* ribosomes and ribosomal subunits active in tRNA binding. *Methods Enzymol 164*:658–670.
Rodnina MV, Wintermeyer W. 1995. GTP consumption of elongation factor Tu during translation of heteropolymeric mRNAs. *Proc Natl Acad Sci USA 92*:1945–1949.
Scott WG, Finch JT, Klug A. 1995. The crystal structure of an all-RNA hammerhead ribozyme: A proposed mechanism for RNA catalytic cleavage. *Cell 81*:995–1002.
Sor F, Fukuhara H. 1984. Erythromycin and spiramycin resistance mutations of yeast mitochondria: Nature of the rib2 locus in the large ribosomal RNA gene. *Nucleic Acids Res 12*:8313–8318.
Steiner G, Kuechler E, Barta A. 1988. Photo-affinity labelling at the peptidyl transferase centre reveals two different positions for the A- and P-sites in domain V of 23S rRNA. *EMBO J 7*:3949–3955.
Stiegler P, Carbon P, Zuker M, Ebel JP, Ehresmann C. 1981. Structural organization of the 16S ribosomal RNA from *E. coli*. Topography and secondary structure. *Nucleic Acids Res 9*:2153–2172.
Streicher B, von Ahsen U, Schroeder R. 1993. Lead cleavage sites in the core structure of group I intron–RNA. *Nucleic Acids Res 21*:311–317.
Streicher B, Wallis MG. 1996. Metal ions as the key to the functioning of both the group I intron and the ribosome. In: Green R, Schroeder R, eds. *Ribosomal RNA and group I introns*. New York: R.G. Landes Company/Chapman & Hall. pp 103–128.
Streicher B, Westhof E, Schroeder R. 1996. The environment of two metal ions surrounding the splice site of a group I intron. *EMBO J 15*:2556–2564.
Varani G. 1995. Exceptionally stable nucleic acid hairpins. *Annu Rev Biophys Biomol Struct 24*:379–404.
Weiss RL, Kimes BW, Morris DR. 1973. Cations and ribosome structure. III. Effects on the 30S and 50S subunits of replacing bound Mg2+ by inorganic cations. *Biochemistry 12*:450–456.
Winter D. 1994. Pb^{2+}-katalysierte spezifische Hydrolyse ribosomaler RNA [thesis]. Vienna: Institute of Biochemistry, University of Vienna.
Winter D, Polacek N, Halama I, Streicher B, Barta A. 1997. Lead-catalysed specific cleavage of ribosomal RNAs. *Nucleic Acids Res 25*:1817–1824.
Woese CR, Winker S, Gutell RR. 1990. Architecture of ribosomal RNA: Constraints on the sequence of "tetra-loops." *Proc Natl Acad Sci USA 87*:8467–8471.
Wower J, Hixson SS, Zimmermann RA. 1989. Labeling the peptidyltransferase center of the *Escherichia coli* ribosome with photoreactive tRNA(Phe) derivatives containing azidoadenosine at the 3′ end of the acceptor arm: A model of the tRNA–ribosome complex. *Proc Natl Acad Sci USA 86*:5232–5236.
Xing Y, Draper DE. 1995. Stabilization of ribosomal RNA tertiary structure by ribosomal protein L11. *J Mol Biol 249*:319–331.
Zhang B, Cech TR. 1997. Peptide bond formation by in vitro selected ribozymes. *Nature 390*:96–100.
Zito K, Huttenhofer A, Pace NR. 1993. Lead-catalyzed cleavage of ribonuclease P RNA as a probe for integrity of tertiary structure. *Nucleic Acids Res 21*:5916–5920.